An electromagnetic study of shell-induced Error Fields and their plasma response in RFX-mod2

A. Corbioli[1,2], D. Abate[1], L. Pigatto[1], M. Brombin[1,3], Y.Q. Liu[4], E. Tomasina[1], F. Villone[5]

[1] *Consorzio RFX (CNR, ENEA, INFN, Università di Padova, Acciaierie Venete SpA), Padova, Italy*

[2] *CRF – Università degli Studi di Padova, Padova, Italy*

[3] *Istituto per la Scienza e la Tecnologia dei Plasmi, CNR, Padova, Italy*

[4] *General Atomics, PO Box 85608, San Diego, 92186-5608, CA, United States of America*

[5] *DIETI, Consorzio CREATE, Università degli Studi di Napoli Federico II, Napoli, Italy*

Introduction RFX-mod2 is a major upgrade of the former RFX-mod machine. The Passive Stabilizing Shell (PSS) is now enclosed within a wider new vacuum vessel and is closer to the plasma: the ratio of shell radius to first wall will decrease from 1.11 of RFX-mod to 1.04 of RFX-mod2, thus improving Magneto-Hydro-Dynamic (MHD) stability[2]. Thanks to flexible power supplies, the active MHD control system, and the upgraded sensors and diagnostics system, RFX-mod2 can operate in both low-current tokamak ($I_p \sim 50 \div 150\,kA$) and large current (I_p up to $2\,MA$) Reversed Field Pinch (RFP) configurations. Moreover, the shaped tokamak operations will be capable of exploring positive and negative triangularity plasmas in "exotic regimes" such as the low-q ($q_a < 2$) and ultra-low-q ($q_a < 1$). In preparation of integrated commissioning and first experiments, a three-dimensional electromagnetic model of the machine has been developed by using the *CARIDDI* code [1]. The model incorporates all the main geometrical features of RFX-mod2, together with all the active coil systems: the Magnetizing and Field Shaping Windings (MWs and FSWs) and the 192 MHD-control-dedicated saddle coils.

Modeling the PSS The main non-axisymmetric feature of RFX-mod2 is the presence of two gaps in the PSS that are located at $\varphi = 123^\circ$ and $\varphi = -57^\circ$. These gaps are required to prevent the circulation of a net toroidal current and to ensure electrical insulation with respect to plasma [2, 3]. However, the resulting break in toroidal symmetry introduces localized error fields associated with the poloidal closure of induced eddy currents. An inner equatorial gap is also present to prevent the circulation of a net poloidal current. The shell has been analyzed using the CARIDDI code[1] which employs a 3D integral formulation for the eddy current problem. In particular, two models have been developed: the simplified butt-joint configuration (BJ) and the realistic double overlap geometry (OL). In the former (Figure 1a) the edges of each toroidal gap are represented as flat, non-overlapping surfaces. The resulting mesh features a poloidal resolution of 6.06° per element, an equatorial gap of 2°, and a toroidal resolution of 6° per element. The two poloidal cuts extend over 1° each. The OL configuration (Figure 1b)

is a more realistic representation of the shell: here the gap region consists of two overlapped sectors of 24° each along the toroidal direction. In order to accurately represent the overlapping geometry, while keeping the numerical complexity manageable, a toroidal resolution of 3° per element has been adopted. For the same reason, second-order 3D features (such as pumping ports and diagnostic openings) have not been included at this stage.

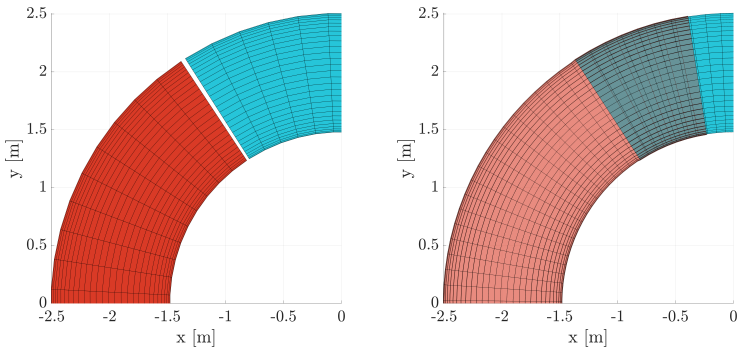

(a) (b)

Figure 1: Top view of the mesh adopted in the BJ (a) and OL (b).

Dynamic Error Field A study has been performed on the magnetic fields generated by the eddy currents on the shell. These fields can be decomposed into an axisymmetric component and a non-axisymmetric component (hereafter referred to as error field B_{ef}). Besides the shell, the model includes also the MW and the FSW, while the plasma current is modeled as a filament centered in $(R_f = 2\ \text{m}, z_f = 0\ \text{m})$. Cariddi formulates the eddy current problem as follows:

$$\begin{bmatrix} \mathbf{L}_{pp} & \mathbf{L}_{pa} \\ \mathbf{L}_{ap} & \mathbf{L}_{aa} \end{bmatrix} \begin{bmatrix} \dot{\mathbf{I}}_p \\ \dot{\mathbf{I}}_a \end{bmatrix} + \begin{bmatrix} \mathbf{R}_p & \mathbb{0} \\ \mathbb{0} & \mathbf{R}_a \end{bmatrix} \begin{bmatrix} \mathbf{I}_p \\ \mathbf{I}_a \end{bmatrix} = \mathbb{0} \tag{1}$$

where the subscripts "p" refers to all the currents in the passive shell, while the subscript "a" refers to the active coils, namely the MW, the FSW and the plasma. From equation (1), the problem is rewritten in state space form, where the state $\mathbf{x} = \mathbf{L}_{pp}\mathbf{I}_p + \mathbf{L}_{pa}\mathbf{I}_a$ is the vector of the fluxes linked with the passive structures:

$$\dot{\mathbf{x}} = \underbrace{-\mathbf{R}_p\mathbf{L}_{pp}^{-1}}_{\mathbf{A}}\ \mathbf{x} + \underbrace{\mathbf{R}_p\mathbf{L}_{pp}^{-1}\mathbf{L}_{pa}}_{\mathbf{B}}\ \mathbf{I}_a\,. \tag{2}$$

Equation (2) allows for the formulation of an initial value problem, where the vector $\mathbf{I}_a$ follows the real time evolution of the currents in the ramp-up of RFX-mod shot #29262, an RFP shot with plasma current reaching 2 MA. The radial component of the magnetic field computed at a set of points is considered to be the output of the system. These virtual sensors are located inside the shell and are arranged on a grid of 120×30 (toroidal $\times$ poloidal) elements in the BJ configuration and of 360×30 elements in the OL configuration.

The error field is time dependent and exhibits two toroidally localized spikes near the gaps (Fig. 2c). We analyzed the two configurations at the respective time instants when the amplitude of the spikes is maximum relative to the local background. In particular, to identify such time instants we used the infinity-norm: we chose $t = t^*$ such that

$$t^* = \arg\max_t \left|\left|\mathbf{B}_{ef}(t)\right|\right|_\infty = \arg\max_t \left|\left|\mathbf{B}_{r,ec}(t) - \mathbf{B}_{r,ec,n=0}(t)\right|\right|_\infty \tag{3}$$

where $\mathbf{B}_{r,ec}(t)$ is the vector of the magnetic fields measured by all the sensors $i = \{1,\dots,n_{sens}\}$, and $\mathbf{B}_{r,ec,n=0}(t)$ is the vector whose i-th entry is the $n = 0$ component of $B_{r,ec,j}(t)$ with $j \in J_i$, $J_i = \{j \in \{1,\dots,n_{sens}\} : \theta_j = \theta_i\}$. The result for OL is 41.3 ms while for BJ is 24.1 ms, in agreement with the analytical estimate (19 ms) [4].

Far from the gaps the shell-induced magnetic field is the same for both configurations. At the BJ gaps, however, this field changes sign compared to the value far-from-the-gaps (Figures 2a and 2c). This implies that, at the gaps, the error field adds to the vacuum field given by the coils: we will refer to this phenomenon as "amplification" and quantify it using the relative error $(B_{gap} - B_{far})/B_{far}$. The amplification is about -2.7, meaning that at the BJ gaps the shell-induced field is ~ 190 mT compared to the far-from-the-gap value of ~ -110 mT. In the OL configuration, the error field at the gap is significantly lower in magnitude and the shell-induced field does not change sign with respect to the far-form-the-gap region (Figures 2b and 2c). In particular, in the overlapped region the amplification is about 0.75, giving a shell-induced field of about -26 mT compared to the far-from-the-gap -105 mT. The overlap reduces the error field magnitude of about 75%, from a spike amplitude of 300 mT for the BJ configuration to 76 mT for the OL configuration.

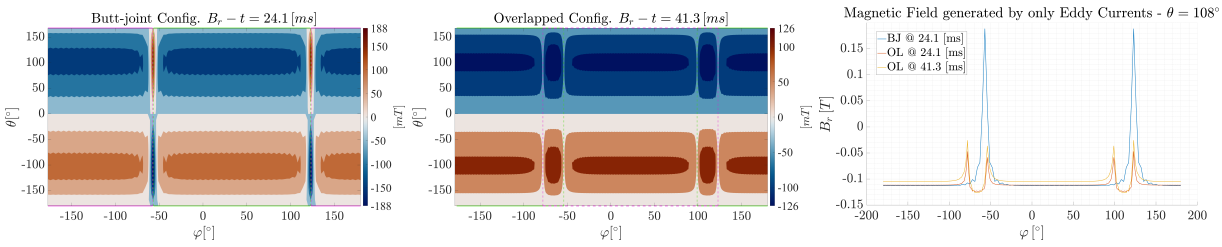

(a) (b) (c)

Figure 2: Eddy current induced radial magnetic field.

Plasma Response The plasma response to the error field in the overlapped configuration has been computed using the MARS-F code [5]. It solves linearized resistive MHD equations in a 2D toroidal geometry. A finite element approach is used in the radial direction while the code is spectral in the poloidal angle. MARS-F can calculate plasma response to external perturbations; in this case the error field is implemented via equivalent surface currents, defined

by mutual inductance coefficients with a coupling surface where the vacuum spectrum is applied. The coupling surface is located in the vacuum region between the grid of virtual sensors and the shell. The surface currents are fixed so that the radial magnetic field generated on the virtual sensors exactly matches the error field obtained from CARIDDI. In order to reduce the numerical complexity, only a subset of the toroidal mode numbers was considered, and a linear combination of single-n responses was performed, thus neglecting the n-coupling. Figure 3 shows the total perturbed field (plasma + vacuum) on the plasma surface. As it can be seen, despite the generated vacuum field being very similar, the plasma response changes drastically depending on whether the $n = 2$ mode is included or not. In this case a kink-like response is dominant, with the typical global pattern even with a relatively local vacuum error field.

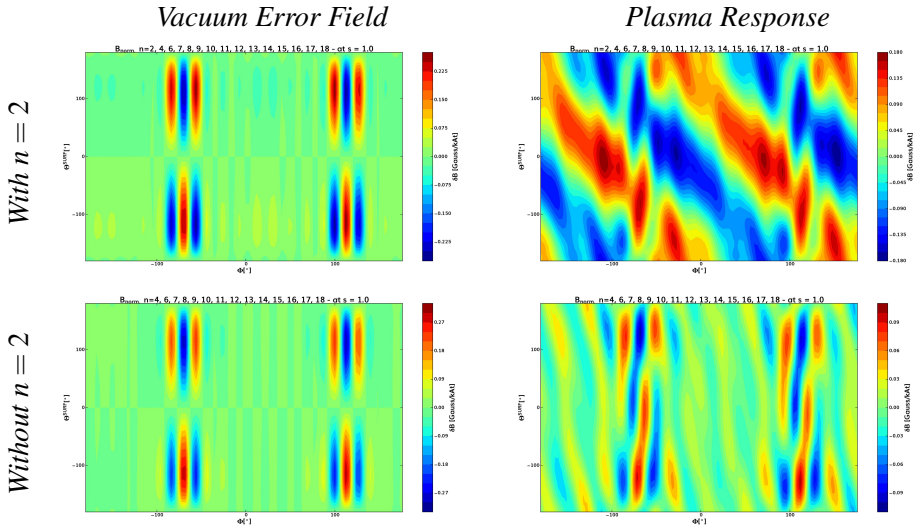

Figure 3: Plasma response in OL configuration @ $t = 41.3$ ms.

Conclusions This study presents the detailed 3D electromagnetic models developed for RFX-mod2, showing the two proposed solutions for the passive stabilizing shell. Far from the gaps, the butt-joint correctly captures the PSS dynamics, but closer to gaps the modeling error becomes unacceptable and the overlapped edge solution must be used. The study confirmed the expected benefits of this geometry [2]. The plasma response of the overlapped configuration shows a dominant non-resonant kink-like pattern ($n = 2$) and a minor resonant spectrum ($n \geq 6$), which will be further investigated.

References

[1] Albanese, R. et al. (1997), "Finite element methods for the solution of 3d eddy current problems" in Advances in Imaging and Electron Physics, Elsevier, 102, 1–86.

[2] Marrelli, L. et al. (2019), *Nucl. Fusion*, 59(7), 076027

[3] Cordaro, L. et al. (2024), *Fus. Eng. Des.*, 207, 114638

[4] Abate, D. et al. (2026), *Plasma Phys. Control. Fusion*, 68(5), 055003

[5] Liu, Y.Q. et al. (2000), *Phys. Plasmas*, 7(9), 3681-3690